US009351674B2

(12) **United States Patent**
Baker, Jr.

(10) **Patent No.: US 9,351,674 B2**
(45) **Date of Patent: *May 31, 2016**

(54) **METHOD FOR ENHANCING PULSE OXIMETRY CALCULATIONS IN THE PRESENCE OF CORRELATED ARTIFACTS**

(71) Applicant: **Covidien LP**, Mansfield, MA (US)

(72) Inventor: **Clark R. Baker, Jr.**, Castro Valley, CA (US)

(73) Assignee: **COVIDIEN LP**, Mansfield, MA (US)

(*) Notice: Subject to any disclaimer, the term of this patent is extended or adjusted under 35 U.S.C. 154(b) by 0 days.

This patent is subject to a terminal disclaimer.

(21) Appl. No.: **14/450,670**

(22) Filed: **Aug. 4, 2014**

(65) **Prior Publication Data**

US 2014/0343385 A1 Nov. 20, 2014

Related U.S. Application Data

(63) Continuation of application No. 13/852,505, filed on Mar. 28, 2013, now Pat. No. 8,818,475, which is a continuation of application No. 12/143,358, filed on Jun. 20, 2008, now Pat. No. 8,423,109, which is a continuation of application No. 11/072,682, filed on Mar. 3, 2005, now Pat. No. 7,392,075.

(51) **Int. Cl.**
A61B 5/1455 (2006.01)
A61B 5/00 (2006.01)
(Continued)

(52) **U.S. Cl.**
CPC ***A61B 5/14551*** (2013.01); ***A61B 5/0205*** (2013.01); ***A61B 5/02416*** (2013.01); ***A61B 5/7207*** (2013.01); ***A61B 5/7214*** (2013.01)

(58) **Field of Classification Search**
CPC A61B 5/1455; A61B 5/14551; A61B 5/14552; A61B 5/7207; A61B 5/7214; A61B 5/0205
See application file for complete search history.

(56) **References Cited**

U.S. PATENT DOCUMENTS

3,638,640 A 2/1972 Shaw
4,714,341 A 12/1987 Hamaguri et al.
(Continued)

FOREIGN PATENT DOCUMENTS

DE 19640807 9/1997
EP 0630203 12/1994
(Continued)

OTHER PUBLICATIONS

Aoyagi, T., et al.; "Analysis of Motion Artifacts in Pulse Oximetry," Japanese Society ME, vol. 42, p. 20 (1993) (Article in Japanese—contains English summary of article).
(Continued)

Primary Examiner — Eric Winakur
(74) *Attorney, Agent, or Firm* — Fletcher Yoder PC

(57) **ABSTRACT**

Methods and systems for determining a physiological parameter in the presence of correlated artifact are provided. One method includes receiving two waveforms corresponding to two different wavelengths of light from a patient. Each of the two waveforms includes a correlated artifact. The method also includes combining the two waveforms to form a plurality of weighted difference waveforms, wherein the plurality of weighted difference waveforms vary from one another by a value of a multiplier. The method further includes identifying one of the weighted difference waveforms from the plurality of weighted difference waveforms using a characteristic of one or more of the plurality of weighted difference waveforms and determining a characteristic of the correlated artifact based at least in part on the identified weighted difference waveform.

19 Claims, 5 Drawing Sheets

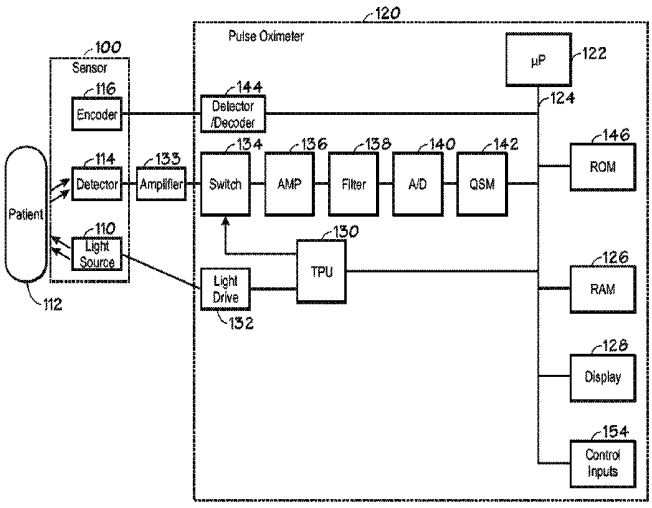

(51) **Int. Cl.**

A61B 5/0205	(2006.01)
A61B 5/024	(2006.01)

(56) **References Cited**

U.S. PATENT DOCUMENTS

4,805,623	A	2/1989	Jöbsis
4,807,631	A	2/1989	Hersh et al.
4,911,167	A	3/1990	Corenman et al.
4,913,150	A	4/1990	Cheung et al.
4,934,372	A	6/1990	Corenman et al.
4,936,679	A	6/1990	Mersh
4,938,218	A	7/1990	Goodman et al.
4,971,062	A	11/1990	Hasebe et al.
4,972,331	A	11/1990	Chance
4,974,591	A	12/1990	Awazu et al.
5,025,791	A	6/1991	Niwa
5,028,787	A	7/1991	Rosenthal et al.
5,065,749	A	11/1991	Hasebe et al.
5,084,327	A	1/1992	Stengel
5,119,815	A	6/1992	Chance
5,122,974	A	6/1992	Chance
5,167,230	A	12/1992	Chance
5,190,038	A	3/1993	Polson et al.
5,226,417	A	7/1993	Swedlow et al.
5,246,003	A	9/1993	DeLonzor
5,247,931	A	9/1993	Norwood
5,263,244	A	11/1993	Genta et al.
5,275,159	A	1/1994	Griebel
5,279,295	A	1/1994	Martens et al.
5,297,548	A	3/1994	Pologe
5,355,880	A	10/1994	Thomas et al.
5,355,882	A	10/1994	Ukawa et al.
5,372,136	A	12/1994	Steuer et al.
5,385,143	A	1/1995	Aoyagi
5,390,670	A	2/1995	Centa et al.
5,413,099	A	5/1995	Schmidt et al.
5,469,845	A	11/1995	DeLonzor et al.
RE35,122	E	12/1995	Corenman et al.
5,482,036	A	1/1996	Diab et al.
5,483,646	A	1/1996	Uchikoga
5,485,847	A	1/1996	Baker, Jr.
5,553,614	A	9/1996	Chance
5,564,417	A	10/1996	Chance
5,575,285	A	11/1996	Takanashi et al.
5,611,337	A	3/1997	Bukta
5,630,413	A	5/1997	Thomas et al.
5,645,059	A	7/1997	Fein et al.
5,645,060	A	7/1997	Yorkey
5,680,857	A	10/1997	Pelikan et al.
5,692,503	A	12/1997	Kuenstner
5,730,124	A	3/1998	Yamauchi
5,743,263	A	4/1998	Baker, Jr.
5,758,644	A	6/1998	Diab et al.
5,779,631	A	7/1998	Chance
5,782,757	A	7/1998	Diab et al.
5,786,592	A	7/1998	Hök
5,830,136	A	11/1998	Delonzor et al.
5,830,139	A	11/1998	Abreu
5,831,598	A	11/1998	Kauffert et al.
5,842,981	A	12/1998	Larsen et al.
5,853,364	A	12/1998	Baker, Jr. et al.
5,871,442	A	2/1999	Madarasz et al.
5,873,821	A	2/1999	Chance et al.
5,920,263	A	7/1999	Huttenhoff et al.
5,924,980	A	7/1999	Coetzee
5,995,855	A	11/1999	Kiani et al.
5,995,856	A	11/1999	Mannheimer et al.
5,995,859	A	11/1999	Takahashi
6,011,986	A	1/2000	Diab et al.
6,064,898	A	5/2000	Aldrich
6,081,742	A	6/2000	Amano et al.
6,083,172	A	7/2000	Baker, Jr. et al.
6,088,607	A	7/2000	Diab et al.
6,094,592	A	7/2000	Yorkey et al.
6,120,460	A	9/2000	Abreu
6,134,460	A	10/2000	Chance
6,135,952	A	10/2000	Coetzee
6,150,951	A	11/2000	Olejniczak
6,154,667	A	11/2000	Miura et al.
6,163,715	A	12/2000	Larsen et al.
6,181,958	B1	1/2001	Steuer et al.
6,181,959	B1	1/2001	Schöllermann et al.
6,230,035	B1	5/2001	Aoyagi et al.
6,266,546	B1	7/2001	Steuer et al.
6,285,895	B1	9/2001	Ristolainen et al.
6,312,393	B1	11/2001	Abreu
6,334,065	B1 *	12/2001	Al-Ali A61B 5/14551 600/323
6,353,750	B1	3/2002	Kimura et al.
6,397,091	B2	5/2002	Diab et al.
6,408,198	B1	6/2002	Hanna et al.
6,411,833	B1	6/2002	Baker, Jr. et al.
6,415,236	B2	7/2002	Kobayashi et al.
6,419,671	B1	7/2002	Lemberg
6,430,525	B1	8/2002	Weber et al.
6,438,399	B1	8/2002	Kurth
6,461,305	B1	10/2002	Schnall
6,463,311	B1	10/2002	Diab
6,466,809	B1	10/2002	Riley
6,487,439	B1	11/2002	Skladnev et al.
6,501,974	B2	12/2002	Huiku
6,501,975	B2	12/2002	Diab et al.
6,505,060	B1	1/2003	Norris
6,510,329	B2	1/2003	Heckel
6,519,486	B1	2/2003	Edgar, Jr. et al.
6,526,301	B2	2/2003	Larsen et al.
6,544,193	B2	4/2003	Abreu
6,546,267	B1	4/2003	Sugiura et al.
6,549,795	B1	4/2003	Chance
6,574,491	B2	6/2003	Elghazzawi
6,580,086	B1	6/2003	Schulz et al.
6,591,122	B2	7/2003	Schmitt
6,594,512	B2	7/2003	Huang
6,594,513	B1	7/2003	Jobsis et al.
6,606,509	B2	8/2003	Schmitt
6,606,511	B1	8/2003	Ali et al.
6,615,064	B1	9/2003	Aldrich
6,618,042	B1	9/2003	Powell
6,622,095	B2	9/2003	Kobayashi et al.
6,654,621	B2	11/2003	Palatnik et al.
6,654,624	B2	11/2003	Diab et al.
6,658,276	B2	12/2003	Kiani et al.
6,658,277	B2	12/2003	Wasserman
6,662,030	B2	12/2003	Khalil et al.
6,668,183	B2	12/2003	Hicks et al.
6,671,526	B1	12/2003	Aoyagi et al.
6,671,528	B2	12/2003	Steuer et al.
6,678,543	B2	1/2004	Diab et al.
6,684,090	B2	1/2004	Ali et al.
6,690,958	B1	2/2004	Walker et al.
6,697,658	B2	2/2004	Al-Ali
6,708,048	B1	3/2004	Chance
6,711,424	B1	3/2004	Fine et al.
6,711,425	B1	3/2004	Reuss
6,714,245	B1	3/2004	Ono
6,721,584	B2	4/2004	Baker, Jr.
6,731,274	B2	5/2004	Powell
6,785,568	B2	8/2004	Chance
6,793,654	B2	9/2004	Lemberg
6,801,797	B2	10/2004	Mannheimer et al.
6,801,798	B2	10/2004	Geddes et al.
6,801,799	B2	10/2004	Mendelson
6,810,277	B2	10/2004	Edgar, Jr. et al.
6,816,741	B2	11/2004	Diab
6,829,496	B2	12/2004	Nagai et al.
6,836,679	B2	12/2004	Baker, Jr. et al.
6,850,053	B2	2/2005	Daalmans et al.
6,863,652	B2	3/2005	Huang et al.
6,873,865	B2	3/2005	Steuer et al.
6,889,153	B2	5/2005	Dietiker
6,898,451	B2	5/2005	Wuori
6,930,608	B2	8/2005	Grajales et al.
6,931,269	B2	8/2005	Terry
6,939,307	B1	9/2005	Dunlop

(56) **References Cited**

U.S. PATENT DOCUMENTS

6,947,780	B2	9/2005	Scharf
6,949,081	B1	9/2005	Chance
6,961,598	B2	11/2005	Diab
6,983,178	B2	1/2006	Fine et al.
6,993,371	B2	1/2006	Kiani et al.
6,996,427	B2	2/2006	Ali et al.
6,999,904	B2	2/2006	Weber et al.
7,016,715	B2	3/2006	Stetson
7,024,233	B2	4/2006	Ali
7,024,235	B2	4/2006	Melker et al.
7,027,849	B2	4/2006	Al-Ali
7,030,749	B2	4/2006	Al-Ali
7,035,679	B2	4/2006	Addison et al.
7,035,697	B1	4/2006	Brown
7,039,538	B2	5/2006	Baker, Jr.
7,044,918	B2	5/2006	Diab
7,047,056	B2	5/2006	Hannula et al.
7,072,702	B2	7/2006	Edgar, Jr. et al.
7,127,278	B2	10/2006	Melker et al.
7,162,306	B2	1/2007	Caby et al.
7,194,293	B2	3/2007	Baker, Jr. et al.
7,209,774	B2	4/2007	Baker, Jr.
7,209,775	B2	4/2007	Bae et al.
7,215,984	B2	5/2007	Diab et al.
7,215,986	B2	5/2007	Diab et al.
7,236,811	B2	6/2007	Schmitt
7,263,395	B2	8/2007	Chan et al.
7,272,426	B2	9/2007	Schmid
7,282,723	B2	10/2007	Schomacker et al.
7,302,284	B2	11/2007	Baker, Jr. et al.
7,315,753	B2	1/2008	Baker, Jr. et al.
7,328,053	B1	2/2008	Diab et al.
7,336,982	B2	2/2008	Yoo
7,336,983	B2	2/2008	Baker, Jr. et al.
7,373,193	B2	5/2008	Al-Ali et al.
7,376,453	B1	5/2008	Diab et al.
7,383,070	B2	6/2008	Diab et al.
7,474,907	B2	1/2009	Baker, Jr.
2001/0005773	A1	6/2001	Larsen et al.
2001/0020122	A1	9/2001	Steuer et al.
2001/0039376	A1	11/2001	Steuer et al.
2001/0044700	A1	11/2001	Kobayashi et al.
2002/0026106	A1	2/2002	Khalil et al.
2002/0035318	A1	3/2002	Mannheimer et al.
2002/0038079	A1	3/2002	Steuer et al.
2002/0042558	A1	4/2002	Mendelson
2002/0049389	A1	4/2002	Abreu
2002/0062071	A1	5/2002	Diab et al.
2002/0111748	A1	8/2002	Kobayashi et al.
2002/0133068	A1	9/2002	Huiku
2002/0156354	A1	10/2002	Larson
2002/0161287	A1	10/2002	Schmitt
2002/0161290	A1	10/2002	Chance
2002/0165439	A1	11/2002	Schmitt
2002/0198443	A1	12/2002	Ting
2003/0023140	A1	1/2003	Chance
2003/0055324	A1	3/2003	Wasserman
2003/0060693	A1	3/2003	Monfre et al.
2003/0097049	A1	5/2003	Diab et al.
2003/0139687	A1	7/2003	Abreu
2003/0144584	A1	7/2003	Mendelson
2003/0187337	A1	10/2003	Tarassenko et al.
2003/0220548	A1	11/2003	Schmitt
2003/0220576	A1	11/2003	Diab
2004/0010188	A1	1/2004	Wasserman
2004/0054270	A1	3/2004	Pewzner et al.
2004/0087846	A1	5/2004	Wasserman
2004/0107065	A1	6/2004	Al-Ali
2004/0127779	A1	7/2004	Steuer et al.
2004/0158135	A1	8/2004	Baker, Jr. et al.
2004/0171920	A1	9/2004	Mannheimer et al.
2004/0176670	A1	9/2004	Takamura et al.
2004/0176671	A1	9/2004	Fine et al.
2004/0181134	A1	9/2004	Baker, Jr. et al.
2004/0204636	A1	10/2004	Diab et al.
2004/0230106	A1	11/2004	Schmitt et al.
2005/0033129	A1	2/2005	Edgar, Jr. et al.
2005/0049470	A1	3/2005	Terry
2005/0080323	A1	4/2005	Kato
2005/0085735	A1	4/2005	Baker, Jr. et al.
2005/0101850	A1	5/2005	Parker
2005/0113651	A1	5/2005	Wood et al.
2005/0113656	A1	5/2005	Chance
2005/0143634	A1	6/2005	Baker, Jr. et al.
2005/0168722	A1	8/2005	Forstner et al.
2005/0177034	A1	8/2005	Beaumont
2005/0192488	A1	9/2005	Bryenton et al.
2005/0197552	A1	9/2005	Baker, Jr.
2005/0197793	A1	9/2005	Baker, Jr.
2005/0203357	A1	9/2005	Debreczeny et al.
2005/0209517	A1	9/2005	Diab et al.
2005/0228248	A1	10/2005	Dietiker
2005/0267346	A1	12/2005	Faber et al.
2005/0283059	A1	12/2005	Iyer et al.
2006/0009688	A1	1/2006	Lamego et al.
2006/0015021	A1	1/2006	Cheng
2006/0020181	A1	1/2006	Schmitt
2006/0030763	A1	2/2006	Mannheimer et al.
2006/0052680	A1	3/2006	Diab
2006/0058683	A1	3/2006	Chance
2006/0064024	A1	3/2006	Schnall
2006/0122476	A1	6/2006	Van Slyke
2006/0161389	A1	7/2006	Weber et al.
2006/0195025	A1	8/2006	Ali et al.
2006/0195028	A1	8/2006	Hannula et al.
2006/0195280	A1	8/2006	Baker, Jr.
2006/0206021	A1	9/2006	Diab
2006/0217609	A1	9/2006	Diab et al.
2006/0224058	A1	10/2006	Mannheimer
2006/0247501	A1	11/2006	Ali
2006/0258921	A1	11/2006	Addison et al.
2006/0258927	A1	11/2006	Edgar, Jr. et al.
2007/0213621	A1	9/2007	Reisfeld et al.
2007/0225581	A1	9/2007	Diab et al.
2007/0249918	A1	10/2007	Diab et al.
2007/0291832	A1	12/2007	Diab et al.
2008/0004514	A1	1/2008	Diab et al.
2008/0033266	A1	2/2008	Diab et al.
2008/0045823	A1	2/2008	Diab et al.

FOREIGN PATENT DOCUMENTS

EP	1006863	10/2003
EP	1006864	10/2003
EP	1491135	12/2004
JP	3170866	7/1991
JP	3238813	10/1991
JP	4191642	7/1992
JP	4332536	11/1992
JP	7124138	5/1995
JP	7136150	5/1995
JP	2003194714	7/2003
JP	2003210438	7/2003
JP	2003275192	9/2003
JP	2003339678	12/2003
JP	2004008572	1/2004
JP	2004113353	4/2004
JP	2004135854	5/2004
JP	2004194908	7/2004
JP	2004202190	7/2004
JP	2004248819	9/2004
JP	2004290545	10/2004
WO	9101678	2/1991
WO	9221281	12/1992
WO	9309711	5/1993
WO	9403102	2/1994
WO	9512349	5/1995
WO	9749330	12/1997
WO	9842249	10/1998
WO	9842251	10/1998
WO	9843071	10/1998
WO	9932030	7/1999
WO	0021438	4/2000
WO	0125802	4/2001

(56) **References Cited**

FOREIGN PATENT DOCUMENTS

WO	03000125	1/2003
WO	2004075746	9/2004
WO	2005009221	2/2005

OTHER PUBLICATIONS

Barreto, A.B., et al.; "Adaptive Cancelation of Motion artifact in Photoplethysmographic Blood Volume Pulse Measurements for Exercise Evaluation," IEEE-EMBC and CMBEC—Theme 4: Signal Processing, pp. 983-984 (1995).

Vincente, L.M., et al.; "Adaptive Pre-Processing of Photoplethysmographic Blood Volume Pulse Measurements," pp. 114-117 (1996).

Barnum, P.T., et al.; "Novel Pulse Oximetry Technology Capable of Reliable Bradycardia Monitoring in the Neonate," Respiratory Care, vol. 42, No. 1, p. 1072 (Nov. 1997).

Barreto, Armando B., et al.; "Adaptive LMS Delay Measurement in dual Blood Volume Pulse Signals for Non-Invasive Monitoring," IEEE, pp. 117-120 (1997).

Leahy, Martin J., et al.; "Sensor Validation in Biomedical Applications," IFAC Modelling and Control in Biomedical Systems, Warwick, UK; pp. 221-226 (1997).

Masin, Donald I., et al.; "Fetal Transmission Pulse Oximetry," Proceedings 19th International Conference IEEE/EMBS, Oct. 30-Nov. 2, 1997; pp. 2326-2329.

Plummer, John L., et al.; "Identification of Movement Artifact by the Nellcor N-200 and N-3000 Pulse Oximeters," Journal of clinical Monitoring, vol. 13, pp. 109-113 (1997).

Poets, C. F., et al.; "Detection of movement artifact in recorded pulse oximeter saturation," Eur. J. Pediatr.; vol. 156, pp. 808-811 (1997).

East, Christine E., et al.; "Fetal Oxygen Saturation and Uterine Contractions During Labor," American Journal of Perinatology, vol. 15, No. 6, pp. 345-349 (Jun. 1998).

Edrich, Thomas, et al.; "Can the Blood Content of the Tissues be Determined Optically During Pulse Oximetry Without Knowledge of the Oxygen Saturation?—An In-Vitro Investigation," Proceedings of the 20th Annual International conference of the IEEE Engie in Medicine and Biology Society, vol. 20, No. 6, p. 3072-3075, 1998.

Hayes, Matthew J., et al.; "Quantitative evaluation of photoplethysmographic artifact reduction for pulse oximetry," SPIE, vol. 3570, pp. 138-147 (Sep. 1998).

Hayes, Matthew J., et al.; "Artifact reduction in photoplethysmography," Applied Optics, vol. 37, No. 31, pp. 7437-7446 (Nov. 1998).

Such, Hans Olaf; "Optoelectronic Non-invasive Vascular Diagnostics Using multiple Wavelength and Imaging Approach," Dissertation, (1998).

Rhee, Sokwoo, et al.; "Design of a Artifact-Free Wearable Plethysmographic Sensor," Proceedings of the First joint BMES/EMBS Conference, Oct. 13-16, 1999, Altanta, Georgia, p. 786.

Rheineck-Leyssius, Aart t., et al.; "Advanced Pulse Oximeter Signal Processing Technology Compared to Simple Averaging: I. Effect on Frequency of Alarms in the Operating Room," Journal of clinical Anestesia, vol. 11, pp. 192-195 (1999).

Todd, Bryan, et al.; "The Identification of Peaks in Physiological Signals," Computers and Biomedical Research, vol. 32, pp. 322-335 (1999).

Kaestle, S.; "An Algorithm for Reliable Processing of Pulse Oximetry Signals Under strong Noise Conditions," Dissertation Book, Lubeck University, Germany (1999).

Coetzee, Frans M.; "Noise-Resistant Pulse Oximetry Using a Synthetic Reference Signal," IEEE Transactions on Biomedical Engineering, vol. 47, No. 8, Aug. 2000, pp. 1018-1026.

Goldman, Julian M.; "Masimo Signal Extraction Pulse Oximetry," Journal of Clinical Monitoring and Computing, vol. 16, pp. 475-483 (2000).

Kaestle, S.; "Determining Artefact Sensitivity of New Pulse Oximeters in Laboratory Using Signals Obtained from Patient," Biomedizinische Technik, vol. 45 (2000).

Belal, Suliman Yousef, et al.; "A fuzzy system for detecting distorted plethysmogram pulses in neonates and paediatric patients," Physiol. Meas., vol. 22, pp. 397-412 (2001).

Cysewska-Sobusaik, Anna; "Metrological Problems With noninvasive Transillumination of Living Tissues," Proceedings of SPIE, vol. 4515, pp. 15-24 (2001).

Hayes, Matthew J., et al.; "A New Method for Pulse Oximetry Possessing Inherent Insensitivity to Artifact," IEEE Transactions on Biomedical Engineering, vol. 48, No. 4, pp. 452-461 (Apr. 2001).

Maletras, Francois-Xavier, et al.; "Construction and calibration of a new design of Fiber Optic Respiratory Plethysmograph (FORP)," Optomechanical Design and Engineering, Proceedings of SPIE, vol. 4444, pp. 285-293 (2001).

Chan, K.W., et al.; "17.3: Adaptive Reduction of Motion Artifact from Photoplethysmographic Recordings using a Variable Step-Size LMS Filter," IEEE, pp. 1343-1346 (2002).

Gehring, Harmut, et al.; "The Effects of Motion Artifact and Low Perfusion on the Performance of a New Generation of Pulse Oximeters in Volunteers Undergoing Hypoxemia," Respiratory Care, Vo. 47, No. 1, pp. 48-60 (Jan. 2002).

Gostt, R., et al.; "Pulse Oximetry Artifact Recognition Algorithm for Computerized Anaesthetic Records," Journal of Clinical Monitoring and Computing Abstracts, p. 471 (2002).

Jopling, Michae W., et al.; "Issues in the Laboratory Evaluation of Pulse Oximeter Performance," Anesth Analg, vol. 94, pp. S62-S68 (2002).

Relente, A.R., et al.; "Characterization and Adaptive Filtering of Motion Artifacts in Pulse Oximetry using Accelerometers," Proceedings of the Second joint EMBS/BMES Conference, Houston, Texas, Oct. 23-26, 2002; pp. 1769-1770.

Tremper, K.K.; "A Second Generation Technique for Evaluating Accuracy and Reliability of Second Generation Pulse Oximeters," Journal of Clinical Monitoring and Computing, vol. 16, pp. 473-474 (2000).

Yamaya, Yoshiki, et al.; "Validity of pulse oximetry during maximal exercise in normoxia, hypoxia, and hyperoxia," J. Appl. Physiol., vol. 92, pp. 162-168 (2002).

Yao, Jianchu, et al.; "Design of a Plug-and-Play Pulse Oximeter," Proceedings of the Second Joint EMBS/BMES Conference, Houston, Texas, Oct. 23-26, 2002; pp. 1752-1753.

Aoyagi, Takuo; "Pulse oximetry: its invention, theory, and future," Journal of Anesthesia, vol. 17, pp. 259-266 (2003).

Cyrill, D., et al.; "Adaptive Comb Filter for Quasi-Periodic Physiologic Signals," Proceedings of the 25th Annual International Conference of the IEEE EMBS, Cancun, Mexico, Sep. 17-21, 2003; pp. 2439-2442.

A. Johansson; "Neural network for photoplethysmographic respiratory rate monitoring," Medical & Biological Engineering & Computing, vol. 41, pp. 242-248 (2003).

Lee, C.M., et al.; "Reduction of motion artifacts from photoplethysmographic recordings using wavelet denoising approach," IEEE EMBS Asian-Pacific Conference on Biomedical Engineering, Oct. 20-22, 2003; pp. 194-195.

Lopez-Silva et al., "Near-infrared transmittance pulse oximetry with laser diodes", Journal of Medical Optics 8(3), 525-533 (Jul. 2003).

Stetson, Paul F.; "Determining Heart Rate from Noisey Pulse Oximeter Signals Using Fuzzy Logic," The IEEE International Conference on Fuzzy Systems, St. Louis, Missouri, May 25-28, 2003; pp. 1053-1058.

Addison, Paul S., et al.; "A novel time-frequency-based 3D Lissajous figure method and its application to the determination of oxygen saturation from the photoplethysmogram," Institute of Physic Publishing, Meas. Sci. Technol., vol. 15, pp. L15-L18 (2004).

Matsuzawa, Y., et al.; "Pulse Oximeter," Home Care Medicine, pp. 42-45 (Jul. 2004); (Article in Japanese—contains English summary of article).

Yao, Jianchu, et al.; "A Novel Algorithm to Separate Motion Artifacts from Photoplethysmographic Signals Obtained With a Reflectance Pulse Oximeter," Proceedings of the 26th Annual International conference of the IEEE EMBS, San Francisco, California, Sep. 2004, pp. 2153-2156.

(56) **References Cited**

OTHER PUBLICATIONS

Yan, Yong-sheng, et al.; "Reduction of motion artifact in pulse oximetry by smoothed pseudo Wigner-Ville distribution," Journal of NeuroEngineering and Rehabilitation, vol. 2, No. 3 (9 pages) (Mar. 2005).

Hamilton, Patrick S., et al.; "Effect of Adaptive Motion-Artifact Reduction on QRS Detection," Biomedical Instrumentation & Technology, May-Jun. 2000;34(3):197-202.

J. Huang, et al.; "Low Power Motion Tolerant Pulse Oximetry," Abstracts, A7, p. S103. (undated).

Kim, J.M., et al.; "Signal Processing Using Fourier & Wavelet Transform," Lasers and Electro-Optics, 2001. CLEO/Pacific Rim 2001. The 4th Pacific Rim Conference vol. 2, pp. II-310-II-311 Conference Date: Jul. 15-19, 2001.

P. Lang, et al.; "Signal Identification and Quality Indicator™ for Motion Resistant Pulse Oximetry," Abstracts, A10, p. S105. (undated).

R. Neumann, et al.; "Fourier Artifact suppression Technology Provides Reliable SpO2,," Abstracts, A11, p. S105. (undated).

Odagiri, Y.; "Pulse Wave Measuring Device," Micromechatronics, vol. 42, No. 3, pp. 6-11 (Article in Japanese—contains English summary of article)(undated).

Yamazaki, Nakaji, et al.; "Motion Artifact Resistant Pulse Oximeter (Durapulse PA 2100)," Journal of Oral Cavity Medicine, vol. 69, No. 4, pp. 53 (Article in Japanese—contains English summary of article) (date unknown).

* cited by examiner

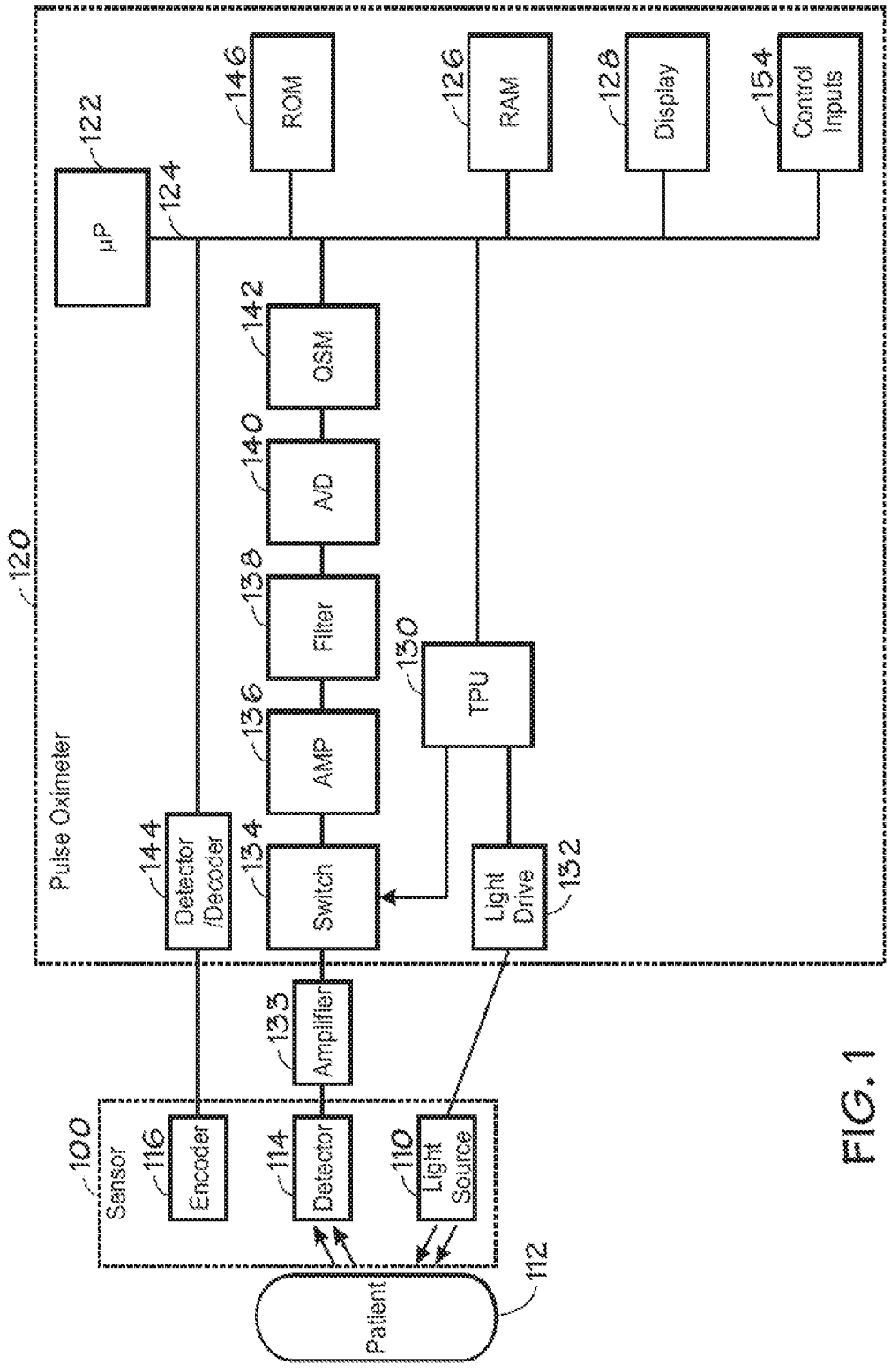
120
Pulse Oximeter
μP
122
124
ROM
146
RAM
126
Display
128
Control Inputs
154
QSM
142
A/D
140
Filter
138
AMP
136
TPU
130
Switch
134
Detector /Decoder
144
Light Drive
132
Amplifier
133
100
Sensor
Encoder
116
Detector
114
Light Source
110
Patient
112

FIG. 1

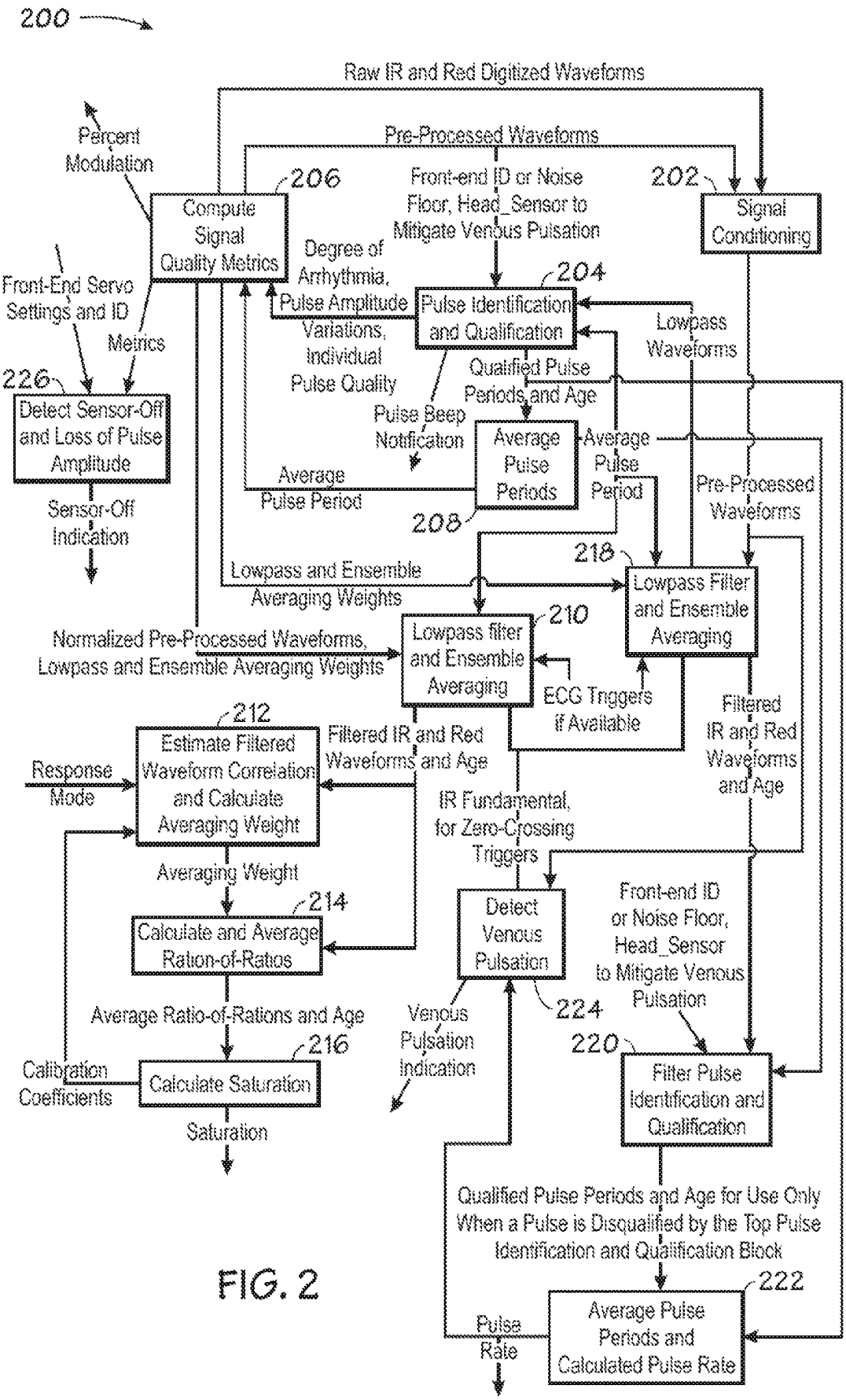
200
Raw IR and Red Digitized Waveforms
Percent Modulation
Pre-Processed Waveforms
206
Front-end ID or Noise Floor, Head_Sensor to Mitigate Venous Pulsation
202
Compute Signal Quality Metrics
Signal Conditioning
Degree of Arrhythmia, Pulse Amplitude Variations, Individual Pulse Quality
204
Front-End Servo Settings and ID
Pulse Identification and Qualification
Lowpass Waveforms
Metrics
Qualified Pulse Periods and Age
226
Pulse Beep Notification
Detect Sensor-Off and Loss of Pulse Amplitude
Average Pulse Periods
Average Pulse Period
Average Pulse Period
Pre-Processed Waveforms
Sensor-Off Indication
208
218
Lowpass and Ensemble Averaging Weights
Lowpass Filter and Ensemble Averaging
210
Normalized Pre-Processed Waveforms, Lowpass and Ensemble Averaging Weights
Lowpass filter and Ensemble Averaging
ECG Triggers if Available
Filtered IR and Red Waveforms and Age
212
Estimate Filtered Waveform Correlation and Calculate Averaging Weight
Filtered IR and Red Waveforms and Age
Response Mode
IR Fundamental, for Zero-Crossing Triggers
Averaging Weight
214
Detect Venous Pulsation
Front-end ID or Noise Floor, Head_Sensor to Mitigate Venous Pulsation
Calculate and Average Ration-of-Ratios
224
Average Ratio-of-Rations and Age
Venous Pulsation Indication
220
216
Calibration Coefficients
Calculate Saturation
Filter Pulse Identification and Qualification
Saturation
Qualified Pulse Periods and Age for Use Only When a Pulse is Disqualified by the Top Pulse Identification and Qualification Block
222
Pulse Rate
Average Pulse Periods and Calculated Pulse Rate

FIG. 2

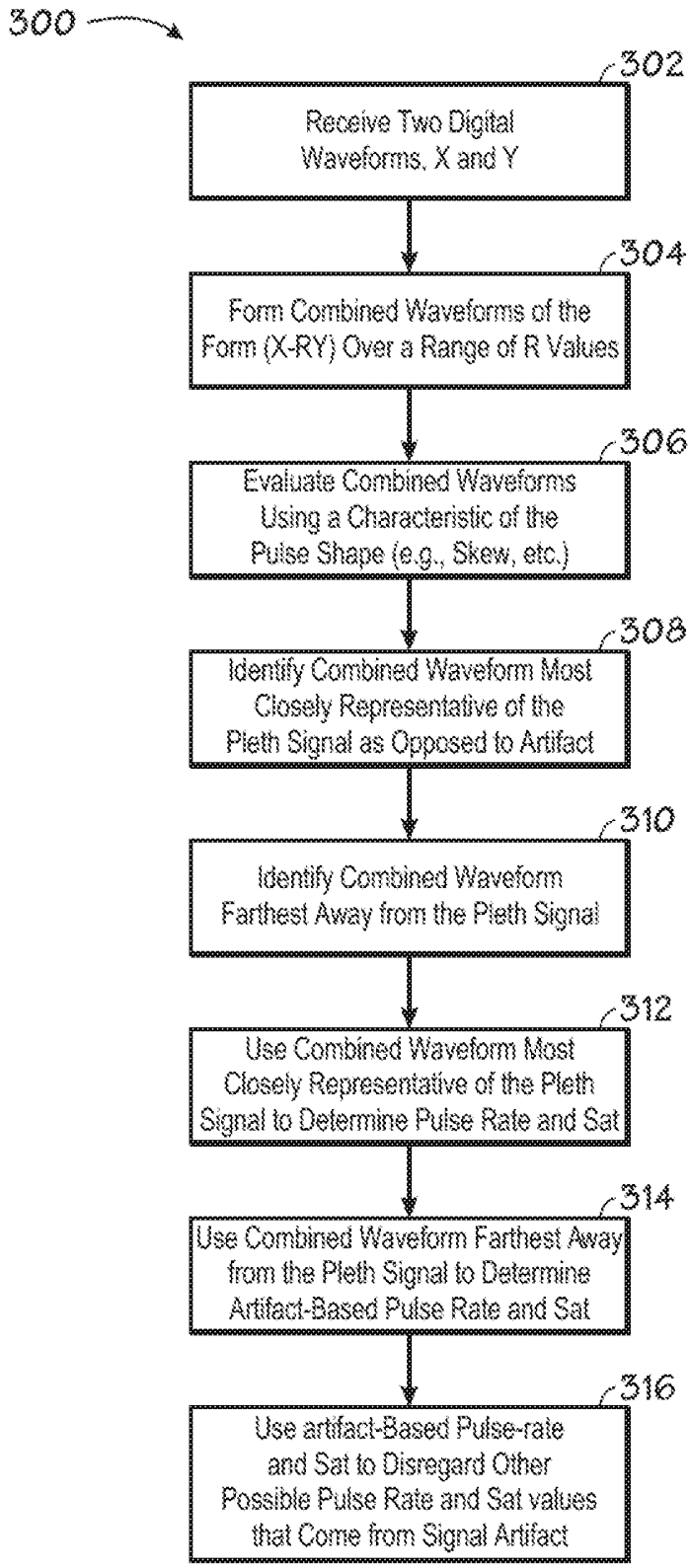
300
302
Receive Two Digital Waveforms, X and Y
304
Form Combined Waveforms of the Form (X-RY) Over a Range of R Values
306
Evaluate Combined Waveforms Using a Characteristic of the Pulse Shape (e.g., Skew, etc.)
308
Identify Combined Waveform Most Closely Representative of the Pleth Signal as Opposed to Artifact
310
Identify Combined Waveform Farthest Away from the Pleth Signal
312
Use Combined Waveform Most Closely Representative of the Pleth Signal to Determine Pulse Rate and Sat
314
Use Combined Waveform Farthest Away from the Pleth Signal to Determine Artifact-Based Pulse Rate and Sat
316
Use artifact-Based Pulse-rate and Sat to Disregard Other Possible Pulse Rate and Sat values that Come from Signal Artifact

FIG. 3

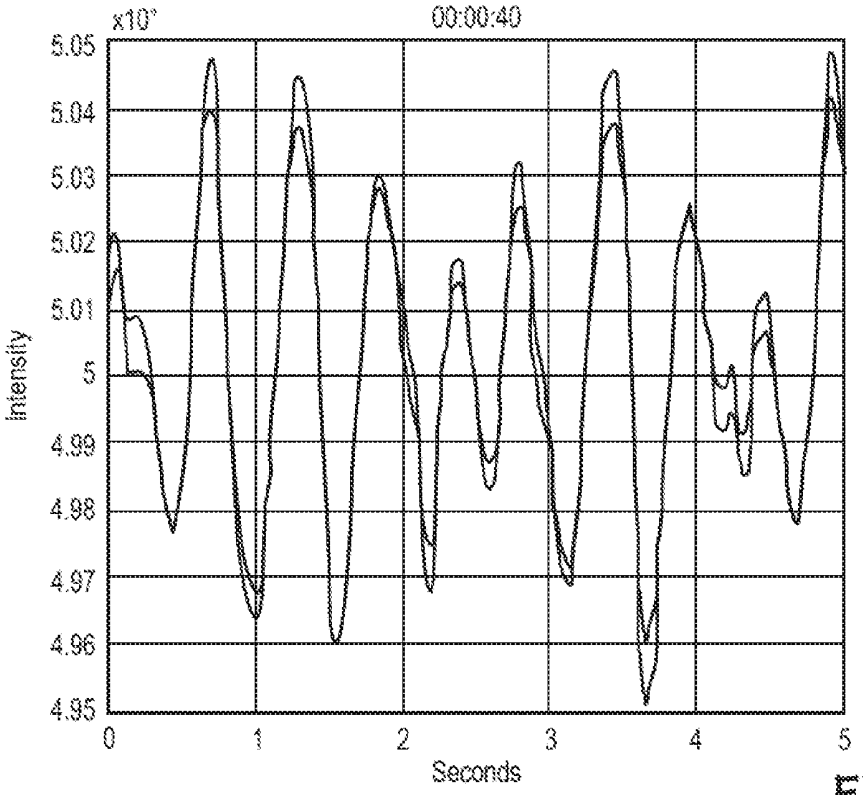
x10^7
00:00:40
5.05
5.04
5.03
5.02
5.01
5
4.99
4.98
4.97
4.96
4.95
Intensity
0
1
2
3
4
5
Seconds

FIG. 4

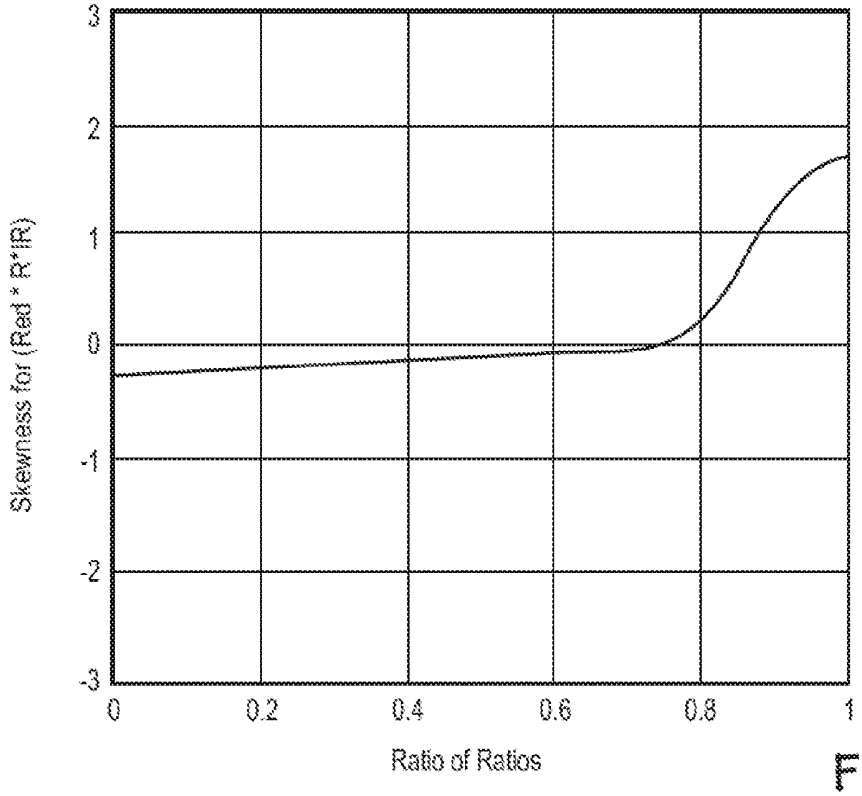
3
2
1
0
-1
-2
-3
Skewness for (Red * R*IR)
0
0.2
0.4
0.6
0.8
1
Ratio of Ratios

FIG. 5

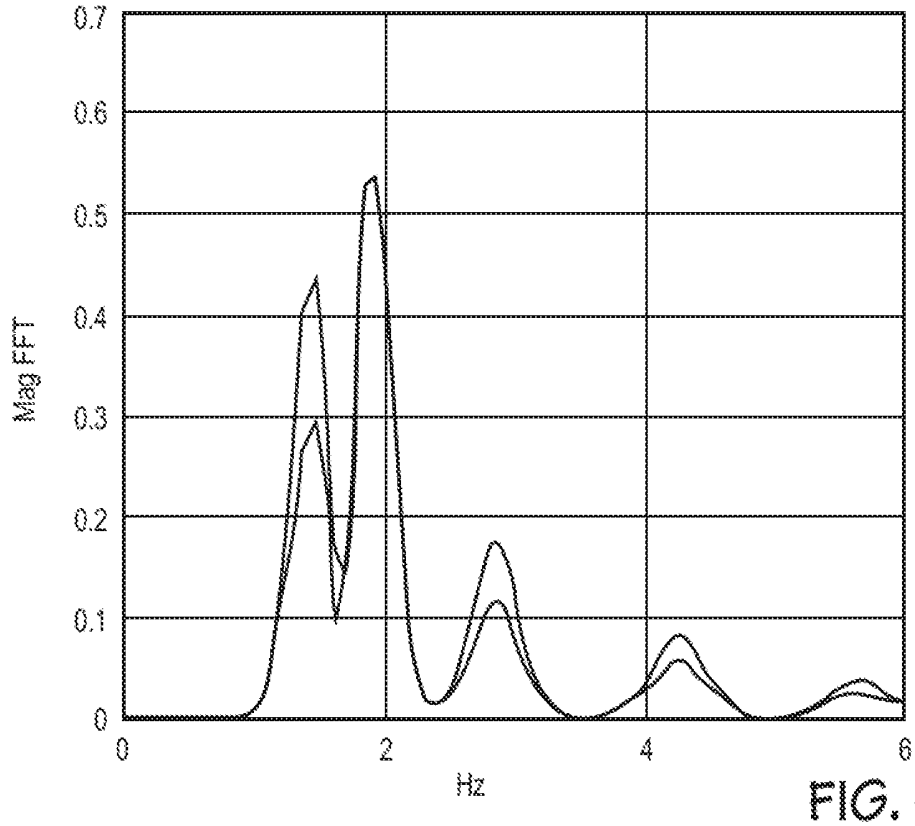
0.7
0.6
0.5
0.4
0.3
0.2
0.1
0
Mag FFT
0
2
4
6
Hz

FIG. 6

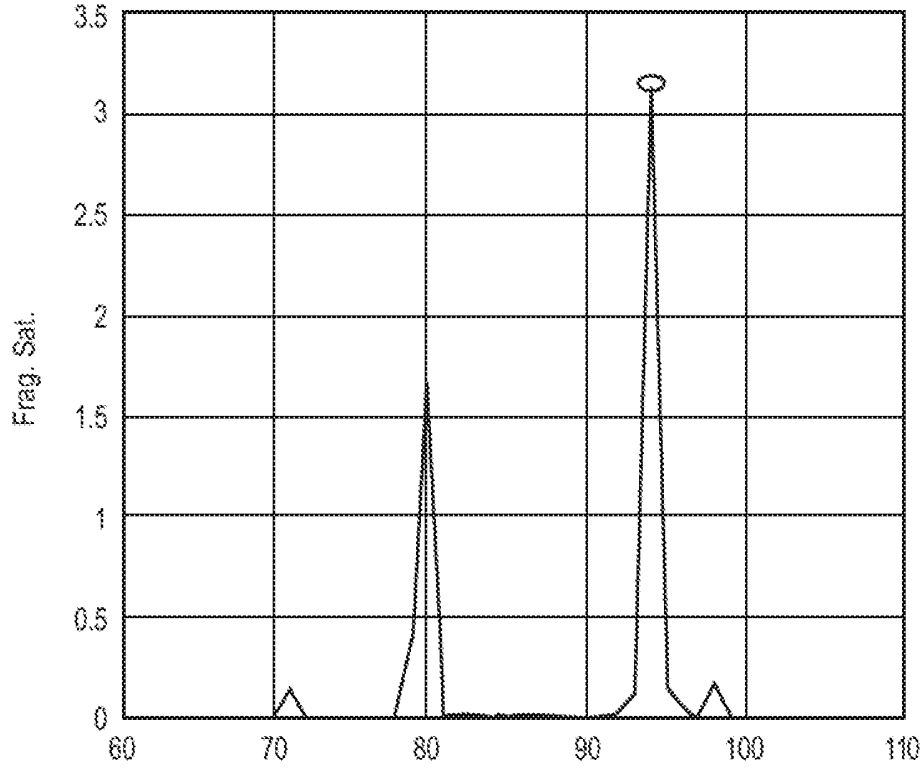
3.5
3
2.5
2
1.5
1
0.5
0
Frag. Sat.
60
70
80
90
100
110

FIG. 7

METHOD FOR ENHANCING PULSE OXIMETRY CALCULATIONS IN THE PRESENCE OF CORRELATED ARTIFACTS

CROSS-REFERENCE TO RELATED APPLICATIONS

This application is a continuation of U.S. application Ser. No. 13/852,505, filed Mar. 28, 2013, which itself is a continuation of Ser. No. 12/143,358, filed Jun. 20, 2008 (U.S. Pat. No. 8,423,109), which itself is a continuation of U.S. application Ser. No. 11/072,682, filed Mar. 3, 2005 (U.S. Pat. No. 7,392,075), the disclosure of which is hereby incorporated by reference in its entirety for all purposes.

BACKGROUND

The present invention relates in general to pulse oximetry, and in particular to the processing of signals generated by a pulse oximeter.

A pulse oximeter is typically used to measure various blood characteristics including the blood oxygen saturation of hemoglobin in arterial blood and the pulse rate of the patient. Measurement of these characteristics has been accomplished by use of a non-invasive sensor that passes light through a portion of a patient's blood perfused tissue and photo-electrically senses the absorption and scattering of light in such tissue. The amount of light absorbed and scattered is then used to estimate the amount of blood constituent in the tissue using various algorithms known in the art. The "pulse" in pulse oximetry comes from the time varying amount of arterial blood in the tissue during a cardiac cycle. The signal processed from the sensed optical measurement is the familiar plethysmographic waveform, which corresponds with the cyclic attenuation of optical energy through a portion of a patient's blood perfused tissue.

Various physiological and/or external factors can adversely impact the accuracy and/or the reliability of physiological parameters that are estimated by a pulse oximeter. These undesirable factors are sometimes referred to as artifacts. Artifacts in general and correlated artifacts in particular can be caused by motion, respiratory artifact, or electronic interference. Correlated artifact is an artifact that perturbs more than one of the signals that are provided by an oximeter sensor, and where the perturbations are largely correlated between those signals.

It is desirable for a pulse oximetry system to be able to perform its calculations in the presence of correlated artifacts.

SUMMARY

The present invention provides a pulse oximeter that has the capability of performing calculations in the presence of correlated artifacts. The embodiments of the present invention provide a method of combining the correlated artifacts from multiple signals so as to cancel or reduce the amplitude of the artifact in the combined signal, wherein the weights for the combining are determined by evaluation of pulse shape characteristics in the combined signal.

In one aspect, the present invention provides a method for determining a physiological parameter in the presence of correlated artifact. The method includes obtaining two digital waveforms, x and y, the waveforms being representative of the absorption of two wavelengths of electromagnetic energy received from a blood-perfused tissue, and where each of the waveforms has a component corresponding to a plethysmographic waveform and a component corresponding to the correlated artifact; calculating several weighted difference waveforms of the form x−R*y, where R is a multiplier, by varying R over a range; evaluating the several weighted difference waveforms using a shape characteristic of the weighted difference waveform; identifying a weighted difference waveform most closely representative of the plethysmographic waveform; identifying a weighted difference waveform most different from the plethysmographic waveform; determining a pleth-based physiological parameter using the waveform most closely representative of the plethysmographic waveform; determining at least one artifact-based physiological parameter using the waveform most different from the plethysmographic waveform; and rejecting other possible candidate values for the pleth-based physiological parameter using the artifact-based physiological parameter.

For a fuller understanding of the nature and advantages of the embodiments of the present invention, reference should be made to the following detailed description taken in conjunction with the accompanying drawings.

BRIEF DESCRIPTION OF THE DRAWINGS

FIG. **1** is a block diagram of an exemplary oximeter.

FIG. **2** is a block diagram of the signal processing architecture of a pulse oximeter in accordance with one embodiment of the present invention.

FIG. **3** is a block diagram of the signal processing architecture of a pulse oximeter in accordance with one embodiment of the present invention for performing calculations in the presence of correlated artifacts.

FIG. **4** is an exemplary graph of IR and Red plethysmograph at a saturation of approximately 94 percent, shown corrupted with a sinusoidal artifacts of equal magnitudes in both channels, which artifacts would yield a saturation of approximately 80 percent.

FIG. **5** is an exemplary graph of skewness of the weighted difference signal.

FIG. **6** is an exemplary FFT graph of IR and Red plethysmograph, reflecting a pulse rate of approximately 85 beats per minutes ("BPM"), with harmonics, and a 115 BPM sinusoid.

FIG. **7** is an exemplary frequency domain histogram of saturation (vs. pulse rate) values obtainable by one of multiple methods. The histogram reflects two potential saturation estimates, one at approximately 80 percent (artifact) and the other at 95 percent (pulse).

DETAILED DESCRIPTION OF THE INVENTION

The methods and systems in accordance with the embodiments of the present invention are directed towards enhancing pulse oximetry calculations in the presence of correlated artifact(s). The invention is particularly applicable to and will be explained by reference to measurements of oxygen saturation of hemoglobin in arterial blood and pulse or heart rate, as in pulse oximeter monitors and pulse oximetry sensors.

A typical pulse oximeter measures two physiological parameters, percent oxygen saturation of arterial blood hemoglobin (SpO_2 or sat) and pulse rate. Oxygen saturation can be estimated using various techniques. In one common technique, the photocurrent generated by the photo-detector is conditioned and processed to determine the ratio of modulation ratios (ratio of ratios) of the red to infrared (IR) signals. This modulation ratio has been observed to correlate well to arterial oxygen saturation. Pulse oximeters and sensors may be empirically calibrated by measuring the modulation ratio over a range of in vivo measured arterial oxygen saturations (SaO_2) on a set of patients, healthy volunteers, or animals.

The observed correlation is used in an inverse manner to estimate blood oxygen saturation (SpO_2) based on the measured value of modulation ratios of a patient. The estimation of oxygen saturation using modulation ratios is described in U.S. Pat. No. 5,853,364, entitled "METHOD AND APPARATUS FOR ESTIMATING PHYSIOLOGICAL PARAMETERS USING MODEL-BASED ADAPTIVE FILTERING," issued Dec. 29, 1998, and U.S. Pat. No. 4,911,167, entitled "METHOD AND APPARATUS FOR DETECTING OPTICAL PULSES," issued Mar. 27, 1990, which are both herein incorporated by reference in their entirety for all purposes. The relationship between oxygen saturation and modulation ratio is described, for example, in U.S. Pat. No. 5,645,059, entitled "MEDICAL SENSOR WITH MODULATED ENCODING SCHEME," issued Jul. 8, 1997, which is herein incorporated by reference in its entirety for all purposes. Most pulse oximeters extract the plethysmographic signal having first determined saturation or pulse rate, both of which are susceptible to interference.

FIG. **1** is a block diagram of one embodiment of a pulse oximeter that may be configured to implement the embodiments of the present invention. Light from light source **110** passes into a blood perfused tissue **112**, and is scattered and detected by photodetector **114**. A sensor **100** containing the light source and photodetector may also contain an encoder **116** which provides signals indicative of the wavelength of light source **110** to allow the oximeter to select appropriate calibration coefficients for calculating oxygen saturation. Encoder **116** may, for instance, be a resistor.

Sensor **100** is connected to a pulse oximeter **120**. The oximeter includes a microprocessor **122** connected to an internal bus **124**. Also connected to the bus are a RAM memory **126** and a display **128**. A time processing unit (TPU) **130** provides timing control signals to light drive circuitry **132** which controls when light source **110** is illuminated, and if multiple light sources are used, the multiplexed timing for the different light sources. TPU **130** also controls the gating-in of signals from photodetector **114** through an amplifier **133** and a switching circuit **134**. These signals are sampled at the proper time, depending upon which of multiple light sources is illuminated, if multiple light sources are used. The received signal is passed through an amplifier **136**, a low pass filter **138**, and an analog-to-digital converter **140**. The digital data is then stored in a queued serial module (QSM) **142**, for later downloading to RAM **126** as QSM **142** fills up. In one embodiment, there may be multiple parallel paths of separate amplifier, filter and A/D converters for multiple light wavelengths or spectra received.

Based on the value of the received signals corresponding to the light received by photodetector **114**, microprocessor **122** will calculate the oxygen saturation using various algorithms. These algorithms require coefficients, which may be empirically determined, corresponding to, for example, the wavelengths of light used. These are stored in a ROM **146**. In a two-wavelength system, the particular set of coefficients chosen for any pair of wavelength spectra is determined by the value indicated by encoder **116** corresponding to a particular light source in a particular sensor **100**. In one embodiment, multiple resistor values may be assigned to select different sets of coefficients. In another embodiment, the same resistors are used to select from among the coefficients appropriate for an infrared source paired with either a near red source or far red source. The selection between whether the near red or far red set will be chosen can be selected with a control input from control inputs **154**. Control inputs **154** may be, for instance, a switch on the pulse oximeter, a keyboard, or a port providing instructions from a remote host computer. Furthermore, any number of methods or algorithms may be used to determine a patient's pulse rate, oxygen saturation or any other desired physiological parameter.

The brief description of an exemplary pulse oximeter set forth above, serves as a basis for describing the methods for enhancing pulse oximetry calculation in the presence of correlated artifact, which are described below.

The embodiments of the present invention may be implemented as a part of a larger signal processing system used to process optical signals for the purposes of operating a pulse oximeter. Such a signal processing system is shown in FIG. **2**, which is a block diagram **200** of a signal processing architecture of a pulse oximeter in accordance with one embodiment of the present invention. The signal processing architecture **200** in accordance with the embodiments of the present invention may be implemented as a software algorithm that is executed by a processor of a pulse oximeter. In addition to calculating oxygen saturation and pulse rate, the system **200** measures various signal metrics that are used to determine filter weighting coefficients. Signal metrics are things that indicate if a pulse is likely a plethysmograph or noise. Signal metrics may be related to, for example, frequency (is it in the range of a human heart rate), shape (is it shaped like a cardiac pulse), rise time, etc. The system shown in FIG. **2** calculates both the oxygen saturation, and the pulse rate, as well as detecting venous pulsation and sensor off and lost pulse conditions, which are described separately below.

I. Oxygen Saturation Calculation

Block **202** represents the operation of the Signal Conditioning block. The digitized red and IR signals or waveforms are received and are conditioned in this block by: (1) taking the 1^{st} derivative to get rid of baseline shift, (2) low pass filtering with fixed coefficients, and (3) dividing by a DC value to preserve the ratio. The function of the Signal Conditioning subsystem is to emphasize the higher frequencies that occur in the human plethysmograph and to attenuate low frequencies in which motion artifact is usually concentrated. The Signal Conditioning subsystem selects its filter coefficients (wide or narrow band) based on hardware characteristics identified during initialization. Inputs to block **202** are digitized red and IR signals, and its outputs are pre-processed red and IR signals.

Block **204** represents the operation of the Pulse Identification and Qualification block. The low pass filtered digitized red and IR signals are provided to this block to identify pulses, and qualify them as likely arterial pulses. This is done using a pre-trained neural network, and is primarily done on the IR signal. The pulse is identified by examining its amplitude, shape and frequency. An input to this block is the average pulse period from block **208**. This function changes the upfront qualification using the pulse rate. The output of block **204** indicates the degree of arrhythmia and individual pulse quality. Inputs to block **204** are: (1) pre-processed red and IR signals, (2) Average pulse period, and (3) lowpass waveforms from the low pass filter. Outputs from block **204** include: (1) degree of arrhythmia, (2) pulse amplitude variations, (3) individual pulse quality, (4) pulse beep notification, and (5) qualified pulse periods and age.

Block **206** is used to compute signal quality metrics. This block (block **206**) determines the pulse shape (e.g., derivative skew), period variability, pulse amplitude and variability, Ratio of Ratios variability, and frequency content relative to pulse rate. Inputs to block **206** include: (1) raw digitized red and IR signals, (2) degree of arrhythmia, individual pulse quality, pulse amplitude variation, (3) pre-processed red and IR signals, and (4) average pulse period. Outputs from block **206** include: (1) lowpass and ensemble averaging filter

weights, (2) metrics for sensor off detector, (3) normalized pre-processed waveforms, and (4) percent modulation.

Block **208** computes average pulse periods. This block (block **208**) calculates the average pulse period from the pulses received. Inputs to block **208** include: qualified pulse periods and age. An output from block **208** includes the average pulse period.

Block **210** represents the functioning of the lowpass filter and ensemble averaging subsystem. Block **210** low pass filters and ensemble averages normalized and preprocessed waveforms processed by block **206**. The weights for the low pass filter are determined by the Signal Metrics block **206**. The signal is also ensemble averaged (this attenuates frequencies other than those of interest near the pulse rate and its harmonics), with the ensemble averaging filter weights also determined by Signal Metrics block **206**. Less weight is assigned if the signal is flagged as degraded. More weight is assigned if the signal is flagged as arrhythmic because ensemble-averaging is not appropriate during arrhythmia. Red and IR waveforms are processed separately, but with the same filtering weights. The filtering is delayed (e.g., approximately one second) to allow the signal metrics to be calculated first.

The filters use continuously variable weights. If samples are not to be ensemble-averaged, then the weighting for the previous filtered samples is set to zero in the weighted average, and the new samples are still processed through the signal processing algorithm. This block tracks the age of the signal and/or the accumulated amount of filtering (e.g., sum of response times and delays in processing). Too old a result will be flagged, if good pulses haven't been detected for a while. The inputs to block **210** include: (1) normalized pre-processed red and IR signals, (2) average pulse period, (3) low pass filter weights and ensemble averaging filter weights, (4) ECG triggers, if available, and (5) IR fundamental, for zero-crossing triggers. Outputs from block **210** include: (1) filtered red and IR signals, and (2) age.

Block **212** represents operations that estimate the ratio-of-ratios variance for the filtered waveforms and calculate averaging weights. The variable weighting for the filter is controlled by the ratio-of-ratios variance. The effect of this variable-weight filtering is that the ratio-of-ratios changes slowly as artifact increases and changes quickly as artifact decreases. The subsystem has two response modes, including fast and normal modes. For example, filtering in the fast mode targets an age metric of 3 seconds, and the target age may be 5 seconds in the normal mode. In the fast mode, the minimum weighting of the current value is clipped at a higher level. In other words, a low weight is assigned to the newest ratio-of-ratios calculation if there is noise present, and a high weight if no noise is present. The inputs to block **212** include: (1) filtered red and IR signals and age, (2) calibration coefficients, and (3) response mode (e.g., user speed settings). Outputs from block **212** include an averaging weight for ratio-of-ratios calculation. The averaging weight is used as an input to block **214** along with filtered IR and Red waveforms to calculate averaged ratio of ratios and age.

Block **216** represents operations that calculate oxygen saturation. Saturation is calculated using an algorithm with the calibration coefficients and averaged ratio of ratios. Inputs to block **116** include: (1) Averaged Ratio-of-Ratios, and (2) calibration coefficients. An output from block **216** is the oxygen saturation value.

II. Pulse Rate Calculation

Block **218** low pass filters and ensemble averages the signal(s) conditioned by block **202**, for the pulse rate identification. The weights for the low pass filter are determined by the Signal Metrics block **206**. The signal is also ensemble averaged (this attenuates frequencies other than those of interest near the pulse rate and its harmonics), with the ensemble averaging filter weights also determined by Signal Metrics block **206**. Less weight is assigned if the signal is flagged as degraded. More weight is assigned if the signal is flagged as arrhythmic because ensemble-averaging is not appropriate during arrhythmia. Red and IR are processed separately, but with the same filtering weights. The filtering is delayed (e.g., approximately one second) to allow the signal metrics to be calculated first.

The filters use continuously variable weights. If samples are not to be ensemble-averaged, then the weighting for the previous filtered samples is set to zero in the weighted average, and the new samples are still processed through the signal processing algorithm. This block (block **218**) tracks the age of the signal and/or the accumulated amount of filtering (sum of response times and delays in processing). Too old a result will be flagged (if good pulses haven't been detected for awhile). Inputs to block **218** include: (1) pre-processed red and IR signals, (2) average pulse period, (3) lowpass filter weights and ensemble averaging filter weights, (4) ECG triggers, if available, and (5) IR fundamental, for zero-crossing triggers. Outputs from block **218** include: (1) filtered red and IR signals and (2) age.

Block **220**, or the Filtered Pulse Identification and Qualification block, calculates the pulse periods from the filtered waveforms, and its results are used only when a pulse is disqualified by block **204**. Inputs to block **220** include: (1) filtered red and IR signals and age, (2) average pulse period, (3) front end ID or noise floor, (4) and the kind or type of sensor that is used to detect the IR and Red energies. Output from block **220** includes qualified pulse periods and age.

Block **222**, or the Average Pulse Periods and Calculate Pulse Rate block, calculates the pulse rate and average pulse period. This block (block **222**) receives qualified pulse periods and age as inputs and provides (1) average pulse period and (2) pulse rate as outputs.

III. Venous Pulsation

Block **224**, or the Detect Venous Pulsation block receives as inputs the pre-processed red and IR signals and age from Block **202**, and pulse rate and provides an indication of venous pulsation as an output. Block **224** also provides an IR fundamental waveform in the time domain using a single-tooth comb filter which is output to the Ensemble Averaging filters (e.g., block **210** and **218**). Inputs to block **224** include: (1) filtered red and IR signals and age and (2) pulse rate. Outputs from block **124** include: an indication of venous pulsation and IR fundamental. In one embodiment, block **224** measures the "openness" of an IR-Red Lissajous plot to determine the whether a flag (e.g., Venous_Pulsation) should be set. The output flag (e.g., Venous_Pulsation) is updated periodically (e.g., every second). In addition, the IR fundamental waveform is output to the Ensemble Averaging filters.

IV. Sensor Off

Block **226**, or the Detect Sensor-Off and Loss of Pulse Amplitude block, uses a pre-trained neural net to determine whether the sensor is off the surface of the blood-perfused tissue, for example, of a patient. The inputs to the neural net are metrics that quantify several aspects of the behavior of the IR and Red values over the last several seconds. Samples are ignored by many of the system **200**'s subsystems while the signal state is either not indicative of a pulse being present, or indicative that a sensor is not on a monitoring site (e.g., Pulse Present, Disconnect, Pulse Lost, Sensor May be Off, and Sensor Off). Inputs to block **226** include: (1) signal quality metrics, and (2) the oximeter's LED brightness, amplifier

gain, and (3) an ID indicating the oximeter's hardware configuration. Outputs from block **226** include a signal state including sensor-off indication.

In the architecture **200** described above, the function of block **226**, Pulse lost and Pulse Search indications, may be derived using information from several parts of the signal processing architecture. In addition, the signal processing architecture will not use the received IR and red waveforms to compute oxygen saturation or pulse rate if a valid sensor is not connected, or if the Sensor-Off or Loss of Pulse Amplitude are detected by the signal processing architecture.

The brief description of an embodiment of a pulse oximeter signal processing architecture in accordance with the present invention, set forth above, serves as a basis for describing the enhanced pulse oximetry calculations in the presence of correlated artifact(s), as is generally depicted by blocks **216** and **222** above.

FIG. **3** is a block diagram **300** of the signal processing architecture of a pulse oximeter in accordance with one embodiment of the present invention for performing enhanced saturation and/or pulse rate calculations in the presence of correlated artifacts. It should be realized that the operations depicted by the diagram **300** need not be carried out in the order shown in FIG. **3**. A person skilled in the art of pulse oximetry signal processing will realize that the operations of FIG. **3** may be carried out in any order, or that steps may be combined, or even skipped. These various permutations of the operation in accordance with the diagram of FIG. **3** are also within the scope of the present methodology. In general, the block diagram **300** shows that in block **302**, two digitized waveforms X and Y are received. In block **304**, the two waveforms are combined to form a weighted difference waveform having the form X−R*Y, where R is a multiplier. The value of R is varied and thus a series of weighted difference waveforms are formed. In block **306**, the combined waveforms are evaluated using a characteristic of the pulse shape. For example, one such pulse shape characteristic is the skew of the combined waveform. In blocks **308** and **310**, the combined waveform most closely representative of a plethysmograph and the waveform least representative of a plethysmograph are identified. Having identified these two waveforms (i.e., most and least representative), the most representative waveforms is used to determine pulse rate and/or oxygen saturation (block **312**). Also, the least representative waveform may optionally be used to determine an artifact-based pulse rate and/or oxygen saturation (block **314**), and the artifact-based estimates of pulse rate and/or oxygen saturation may optionally be used to disregard other possible estimates of pulse rate and/or oxygen saturation (block **316**).

The operation of diagram **300** is described in further detail below. The method for enhancing saturation and/or pulse rate calculation in the presence of correlated artifact, includes the following steps, namely:

1. Calculating two or more digital waveforms, where the two waveforms correspond to the absorption of two or more wavelengths of electromagnetic energy received from a pulsatile tissue bed;

2. Filtering the waveforms to emphasize one or more characteristic of the pulse shape that differentiates the waveform from correlated artifact. For example, applying a first difference filter to a normal or typical human plethysmograph produces a filtered waveform with a skewness between −1 and −2 in most subjects, whereas applying the same filter to a motion artifact signal produces a filtered waveform with a near-zero skewness.

3. Calculating multiple weighted differences between the filtered waveforms, X and Y, of the form X−R*Y.

4. Varying R over a range such that some value of R results in a weighted difference waveform that minimizes the correlated artifact.

5. Calculating the skewness or other shape characteristic of the weighted difference waveforms over an appropriate time interval (e.g., at least one pulse period).

6. Selecting the value of R that produces a weighted difference waveform having a shape that is least characteristic of a pulse. This waveform most closely resembles the artifact.

7. Calculating a saturation value using the waveform of "6" above.

8. Using the saturation value of "7" above for selecting from among multiple saturation estimates calculated by other saturation calculation algorithms.

9. Calculating saturation from the two or more filtered waveforms, but excluding those components contained in the weighted difference waveform having a shape that is least characteristic of a pulse. The exclusion operation may be performed in various ways. For example, the strongest one or more frequencies contained in the least characteristic weighted difference waveform may be the excluded frequencies. Alternatively, the least characteristic waveform (i.e. per "6" above) may be canceled from the two or more filtered waveforms using a cancellation filter.

10. Selecting the weighted difference waveform of "6" above having a skew that is most characteristic of a pulse.

11. Using the weighted difference waveform of "10" above to calculate a pulse rate.

12. Calculating oxygen saturation using the waveform of "10" above and using only those components of the waveform used for calculating the pulse rate. For example, the useful components may be isolated in a manner similar to the exclusion operation of "9" above.

13. Calculating the skewness or other shape characteristic of the weighted difference waveforms over an appropriate time interval (e.g., at least one pulse period), wherein the total absolute difference in skewness between multiple consecutive values over a selected range of R is used as a measure of the complexity of the pulse oximetry signal, where overly complex signals are rejected as unsuitable for oxygen saturation and/or pulse rate calculation.

14. Combining "13" above, and wherein the measure of complexity is applied to other metrics, such as for example, energy, corresponding to the selected range of R, where overly complex signals are rejected as unsuitable for oxygen saturation and/or pulse rate calculation.

The operation of the enhanced signal processing in accordance with the embodiments of the present invention, which is generally described in conjunction with FIG. **3** above, is further described below in conjunction with FIGS. **4-7**.

FIG. **4** is an exemplary graph of IR and Red plethysmograph at a saturation of approximately 94 percent, shown corrupted with a sinusoidal artifacts of equal magnitudes in both channels, which artifacts would yield a saturation of approximately 80 percent.

FIG. **5** is an exemplary graph of skewness of the weighted difference signal.

FIG. **6** is an exemplary FFT graph of IR and Red plethysmograph, reflecting a pulse rate of approximately 85 beats per minutes ("BPM"), with harmonics, and a 115 BPM sinusoid.

FIG. **7** is an exemplary frequency domain histogram of saturation (vs. pulse rate) values obtainable by one of multiple methods. The histogram reflects two potential saturation estimates, one at approximately 80 percent (artifact) and the other at 95 percent (pulse).

In FIG. **5**, the weighted difference waveform (Red—R*IR) having a skewness least-characteristic of a pulse (i.e. zero

skewness) occurs for R of approximately 0.7, or a saturation value of approximately 92 percent, which corresponds with the saturation estimate that is made using the method of step 7 above. In step 8, this value of R is used to select the saturation value of 94 percent from the saturation histogram of FIG. **7**, and not the possible saturation value of 80 percent (from the saturation histogram of FIG. **7**). Using the complexity metrics described in step 13 (i.e., the skewness graph of FIG. **5**) and step 14 (for the saturation histogram of FIG. **7**) both indicate that the IR and Red waveforms are suitable for pulse oximetry calculations, containing only two primary components, of which only one has a characteristic pulse shape.

In FIG. **5**, the weighted difference waveform (Red—R*IR) having a skewness most-characteristic of a pulse (i.e., a very non-zero skewness) occurs for R of approximately 0.1, which resulting weighted difference waveform is the inversion of the plethysmograph, and no artifact. This most characteristic waveform may be used to reliably calculate pulse rate in "11," above. In addition, a filter may be used to extract the components of the most-characteristic waveform from the two or more waveforms of "2" above, for use in saturation calculation per "12" above.

In some embodiments of the present invention, pulse shape metrics other than the skewness may be used for the processing of the waveforms. These other metrics include various signal quality metrics described above in conjunction with Block **206** of FIG. **2**. In particular, other pulse shape metrics may include: the pulse shape (e.g., derivative skew), period variability, pulse amplitude and variability, Ratio of Ratios variability, and frequency content relative to pulse rate, degree of arrhythmia, individual pulse quality, pulse amplitude variation, the degree of similarity or correlation between the two waveforms, the degree of motion artifact by obtaining a ratio of a current pulse amplitude to the long-term average pulse amplitude of said signals, a ratio of a current pulse amplitude to the previous pulse amplitude, and a ratio of a current pulse period to that of an average pulse period. In addition, other pulse shape metrics such as, the "MIN-MAX-MIN" and the "PATH LENGTH" pulse shape indicators, may also be used.

The "MIN-MAX-MIN" indicator provides for a measure of the arterial pulse shape. The arterial pulse referred to herein is caused by a cardiac cycle commonly referred to a heartbeat. During a typical cardiac cycle, blood pressure rises from a minimum value (MIN) at diastole to a maximum (MAX) at systole. The "MIN-MAX-MIN" indicator is a ratio represented by a fraction having the time it takes the pulse to go from a MAX to a MIN as the numerator and having the time it takes the pulse to go from a MIN to a MAX as the denominator. This indicator provides an indication of the ratio of fall to rise times of arterial pulse. A fundamental fact of human physiology is that in a typical arterial pulse, it takes a shorter time to go from the diastole to systole (MIN to MAX) than it does to go from systole to diastole (MAX to MIN). Recognizing this fundamental physiological aspect, then if the "MIN-MAX-MIN" indicator shows that for a pulse, the rise time is bigger than the fall time, then this indicates that the sensor's light is being modulated by other than an arterial pulse. The inventor herein has identified that when a pulse's rise time is bigger than its fall time, the light is not modulated by pulsation of evenly distributed arterial blood, but it is most likely that the observed pulse-like phenomenon is due to throbbing of underlying large blood vessels or physical movement of the sensor. It is known that either of these mechanisms may cause large errors in the calibration of the resulting oxygen saturation estimate. Therefore, by analyzing the shape of the arterial pulse, the "MIN-MAX-MIN" indicator determines whether the light modulation is due to a pulsation, or evenly distributed arterial blood, or other phenomenon such as motion.

The "PATH LENGTH" indicator is also indicative of the pulse shape. This indicator provides for a measure of the frequency content of the pulse waveform relative to the pulse rate. While many algorithms may be used to compute "PATH LENGTH," one equation that may be used to compute it is as follows:

$$PathLength = \frac{\sum_{i=0}^{i=Samples\_in\_Pulse-1} |IR_{t-i} - IR_{t-i-1}|}{Pulse\_Max - Pulse\_Min}$$

High values of this metric indicate that a high proportion of the energy in the pulse is at frequencies higher than the pulse rate. High frequency components in the arterial pulse shape are an indication that light is being modulated by other than arterial pulsations. These high frequency components are also most likely to be caused by movement of the sensor. As described above, it is known that physical movement is a source of error when estimating blood oxygen saturation in pulse oximeters. Therefore, the "PATH LENGTH" indicator, is also a motion and/or pulse shape indicator, which is used to infer that signals that have high frequency components often lead to inaccurate estimates of pulse rate and/or blood oxygen saturation.

Accordingly, as will be understood by those of skill in the art, the present invention which is related to enhancing pulse oximetry calculations in the presence of correlated artifact(s), may be embodied in other specific forms without departing from the essential characteristics thereof. For example, while some aspects of the present embodiments have been described in the time-domain, frequency-based methods are equally relevant to the embodiments of the present invention. Accordingly, the foregoing disclosure is intended to be illustrative, but not limiting, of the scope of the invention, which is set forth in the following claims.

What is claimed is:

1. A medical monitor, comprising:

a light drive configured to drive one or more light emitters;

circuitry configured to receive signals from one or more photodetectors, wherein the signals comprise a correlated artifact;

a memory storing instructions configured to:

combine the plurality of received signals to form a plurality of weighted difference waveforms;

identify a weighted difference waveform from the plurality of weighted difference waveforms that most or least closely resembles a plethysmographic waveform; and

determine a physiological parameter based at least in part on the identified weighted difference waveform; and

a processor configured to execute the instructions.

2. The medical monitor of claim **1**, wherein the memory stores instructions configured to identify a weighted difference waveforms from the plurality of weighted difference waveforms by identifying the waveform that least closely resembles a plethysmographic waveform.

3. The medical monitor of claim **2**, wherein the memory stores instructions configured to determine a least representative physiological parameter based at least in part on the waveform that least closely resembles a plethysmographic waveform.

4. The medical monitor of claim 3, wherein the memory stores instructions configured to identify physiological parameter measurements that are associated with the correlated artifact.

5. The medical monitor of claim 4, wherein the memory stores instructions configured to disregard physiological parameter measurements that are associated with the correlated artifact when determining the physiological parameter.

6. The medical monitor of claim 1, wherein the correlated artifact comprises an artifact caused by patient motion, a respiratory artifact, an electronic interference artifact, or a combination thereof.

7. A pulse oximetry system comprising:

a sensor configured to detect electromagnetic radiation signals corresponding to different wavelengths of light; and

a processor configured to:

receive the signals corresponding to the different wavelengths of light from the sensor;

combine the signals to form a plurality of weighted difference waveforms that vary by a multiplier;

determine a physiological parameter measurement based at least in part on the plurality of weighted difference waveforms; and

determine that the physiological parameter is valid based on its association with a waveform of the plurality of weighted difference waveforms that most closely resembles a plethysmographic waveform.

8. The system of claim 7, wherein the processor is configured to determine the physiological parameter is invalid based on its association with a waveform of the plurality of weighted difference waveforms that least closely resembles a plethysmographic waveform.

9. The system of claim 8, wherein the waveform of the plurality of weighted difference waveforms that least closely resembles a plethysmographic waveform has a characteristic skew associated with an artifact.

10. The system of claim 7, wherein the waveform of the plurality of weighted difference waveforms that most closely resembles a plethysmographic waveform has a skew associated with a pulse.

11. The system of claim 7, wherein the waveform of the plurality of weighted difference waveforms that most closely resembles a plethysmographic waveform has a derivative skew associated with a pulse.

12. The system of claim 7, wherein the waveform of the plurality of weighted difference waveforms that most closely resembles a plethysmographic waveform has a pulse amplitude associated with a pulse.

13. The system of claim 7, wherein the waveform of the plurality of weighted difference waveforms that most closely resembles a plethysmographic waveform has a ratio of ratios variability associated with a pulse.

14. The system of claim 7, wherein the waveform of the plurality of weighted difference waveforms that most closely resembles a plethysmographic waveform has a pulse amplitude variability associated with a pulse.

15. A medical monitor, comprising:

a light drive configured to drive one or more light emitters;

circuitry configured to receive a signal from one or more photodetectors;

a memory storing instructions configured to:

determine a pulse shape parameter of the signal based on a min-max-min indicator, wherein the min-max-min indicator for a pulse corresponds to a ratio of a time from max-min over a time from min-max;

determine if the pulse shape is associated with a valid pulse based on the pulse shape parameter; and

determine a physiological parameter measurement based at least in part on the signal when the signal is associated with the valid pulse; and

a processor configured to execute the instructions.

16. The medical monitor of claim 15, wherein the pulse shape is not associated with a valid pulse when the min-max-min indicator is less than 1.

17. The medical monitor of claim 15, wherein the pulse shape is associated with a valid pulse when the min-max-min indicator is greater than 1.

18. The medical monitor of claim 15, wherein the memory stores instructions configured to identify physiological parameter measurements that are associated with a correlated artifact.

19. The medical monitor of claim 15, wherein the memory stores instructions configured to disregard the signal when the signal is not associated with the valid pulse.

* * * * *

专利名称(译)	在存在相关伪像的情况下增强脉搏血氧测量计算的方法		
公开(公告)号	US9351674	公开(公告)日	2016-05-31
申请号	US14/450670	申请日	2014-08-04
[标]申请(专利权)人(译)	柯惠有限合伙公司		
申请(专利权)人(译)	COVIDIEN LP		
当前申请(专利权)人(译)	COVIDIEN LP		
[标]发明人	BAKER JR CLARK R		
发明人	BAKER, JR., CLARK R.		
IPC分类号	A61B5/1455 A61B5/00 A61B5/0205 A61B5/024		
CPC分类号	A61B5/14551 A61B5/0205 A61B5/02416 A61B5/7207 A61B5/7214		
优先权	12/143358 2013-04-16 US 11/072682 2008-06-24 US		
其他公开文献	US20140343385A1		
外部链接	Espacenet USPTO		

摘要(译)

提供了用于在存在相关伪像的情况下确定生理参数的方法和系统。一种方法包括接收对应于来自患者的两种不同波长的光的两个波形。两个波形中的每一个包括相关伪像。该方法还包括组合两个波形以形成多个加权差分波形，其中多个加权差分波形彼此相乘乘数的值。该方法还包括使用多个加权差异波形中的一个或多个的特征从多个加权差异波形中识别加权差异波形之一，并且至少部分地基于所识别的加权差异来确定相关伪影的特征。波形。